Sialic Acid–Imprinted Fluorescent Core–Shell Particles for Selective Labeling of Cell Surface Glycans

ARTICLE *in* JOURNAL OF THE AMERICAN CHEMICAL SOCIETY · SEPTEMBER 2015

Impact Factor: 12.11 · DOI: 10.1021/jacs.5b08482

9 AUTHORS, INCLUDING:

Zahra El-Schich
Malmö University
8 PUBLICATIONS **57** CITATIONS
SEE PROFILE

Wei Wan
Bundesanstalt für Materialforschung und -prü…
6 PUBLICATIONS **55** CITATIONS
SEE PROFILE

Knut Rurack
Bundesanstalt für Materialforschung und -prü…
139 PUBLICATIONS **6,080** CITATIONS
SEE PROFILE

JACS
JOURNAL OF THE AMERICAN CHEMICAL SOCIETY

Article

pubs.acs.org/JACS

Sialic Acid-Imprinted Fluorescent Core–Shell Particles for Selective Labeling of Cell Surface Glycans

Sudhirkumar Shinde,[†,⊥] Zahra El-Schich,[†] Atena Malakpour,[†] Wei Wan,[‡] Nishtman Dizeyi,[§] Reza Mohammadi,[†,∥] Knut Rurack,[‡] Anette Gjörloff Wingren,[†,⊥] and Börje Sellergren*[,†]

[†]Department of Biomedical Sciences, Faculty of Health and Society, Malmö University, SE-20506 Malmö, Sweden
[‡]Chemical and Optical Sensing Division, Federal Institute for Materials Research and Testing (BAM), 12200 Berlin, Germany
[§]Department of Translational Medicine, Lund University, SE-20502 Malmö, Sweden

Supporting Information

ABSTRACT: The expression of cell surface glycans terminating with sialic acid (SA) residues has been found to correlate with various disease states there among cancer. We here report a novel strategy for specific fluorescence labeling of such motifs. This is based on sialic acid-imprinted core–shell nanoparticles equipped with nitrobenzoxadiazole (NBD) fluorescent reporter groups allowing environmentally sensitive fluorescence detection at convenient excitation and emission wavelengths. Imprinting was achieved exploiting a hybrid approach combining reversible boronate ester formation between *p*-vinylphenylboronic acid and SA, the introduction of cationic amine functionalities, and the use of an NBD-appended urea-monomer as a binary hydrogen-bond donor targeting the SA carboxylic acid and OH functionalities. The monomers were grafted from 200 nm RAFT-modified silica core particles using ethylene glycol dimethacrylate (EGDMA) as cross-linker resulting in a shell thickness of ca. 10 nm. The particles displayed strong affinity for SA in methanol/water mixtures ($K = 6.6 \times 10^5$ M^{-1} in 2% water, 5.9×10^3 M^{-1} in 98% water, $B_{max} \approx 10$ μmol g^{-1}), whereas binding of the competitor glucuronic acid (GA) and other monosaccharides was considerably weaker (K (GA) = 1.8×10^3 M^{-1} in 98% water). In cell imaging experiments, the particles selectively stained different cell lines in correlation with the SA expression level. This was further verified by enzymatic cleavage of SA and by staining using a FITC labeled SA selective lectin.

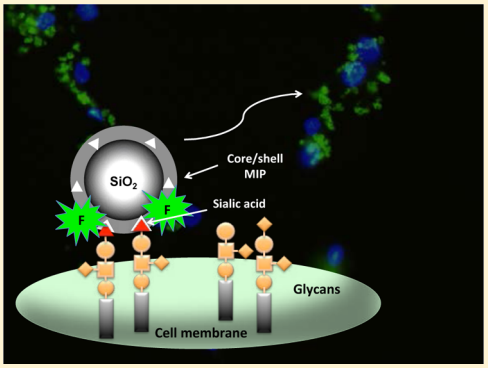

INTRODUCTION

Cell surface glycans refer to a vast variety of glycan motifs attached to plasma membrane bound proteins or lipids.[1] These constitute the outermost surface of the cell and are involved in cellular communication and processes like cellular differentiation, proliferation, and infection. Sialic acid is one of the key constituents in these glycans, and its occurrence has proven to correlate with several disease states such as cardiovascular and neurological diseases and cancer.[2,3] Analyzing and determining these glycosylation motifs is therefore an important diagnostic goal, but the task has proven challenging due to the limited availability of lectins and glycan-specific antibodies.[4,5]

This warrants the development of alternative glycan specific receptors, which could be used for cell imaging, cell sorting, cellular glycosylation analysis, or for the selective inhibition of cell surface interactions.[1,6,7] A plethora of low molecular hosts have been systematically designed for this purpose[7−11] and conjugated, for example, to fluorescent reporter groups[7] or quantum dots[12] for imaging applications. The most powerful hosts for sialic acid feature two or more orthogonal binding groups, a boronic acid directed toward the diol functionality, and a charged or neutral anion receptor directed toward the carboxylate function.[10,13,14] Other strong binders are multifunctional incorporating two or more boronic acid groups.[7] The latter engage in a pH-dependent reversible esterification with the diols resulting in five- or six-membered cyclic structures.[15]

Monosaccharide selective receptors can also be prepared by the technique of molecular imprinting.[16,17] Wulff et al. reported highly discriminative boronate-based receptors for mannose, fructose, and galactose prepared using the monosaccharide templates conjugated to two molecules of vinylbenzeneboronic acid (**1**). Other researchers later adopted this procedure for the synthesis of sialic acid-imprinted bulk polymers or sensor coatings[18,19] featuring strong template affinity when probed in basic buffer/acetonitrile mixtures (pH 8). A simpler one-pot protocol was used for the synthesis of glycoprotein selective solgel coatings[20] and receptors for glycoprotein assays.[21] Here, the boronate monomer is conjugated in situ under base catalysis to the glycoprotein followed by polymerization with a cross-linking monomer to form the imprinted polymer. Even more versatile appears the oriented surface imprinting approach

Received: August 11, 2015

DOI: 10.1021/jacs.5b08482
J. Am. Chem. Soc. XXXX, XXX, XXX−XXX

recently reported by Liu et al. for targetting of individual glycans.[22] The applications of the aforementioned receptors have focused on specific assays of soluble glycoproteins. In contrast, our goal was here to develop SA-imprinted particles of defined size, which could serve as imaging agents of specific cell surface glycan motifs (Figure 1).[23] For this purpose, we decided to build on our previous design of fluorogenic urea-based oxyanion hosts[24] considering the following:

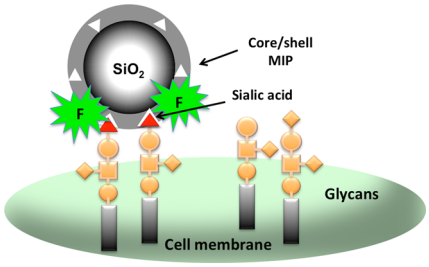

Figure 1. Principle of using MIPs as tools for imaging of sialic acid terminated glycan motifs.

(1) As for the tightest binding hosts for SA, the MIP should incorporate at least two orthogonal binding groups. Recognition in water is best achieved using boronic acids and/or cationic groups, possibly in combination with hydrogen-bond stabilization.

(2) The MIP should exhibit guest responsive fluorescence. For this purpose, we chose the NBD fluorophore, which has been widely used in biological assays and imaging due to its favorable spectroscopic properties.[25]

(3) The MIP format should allow facile tuning of bead size for direct interactions to occur on the cell surface or inside the cell post endocytosis. In this context, the core−shell format appears particularly attractive due to its modular construction.

Hence, in addition to boronic acid **1**, targeting diols C7−C9 or C8−C9 or the α-hydroxy carboxylate functionality, we included urea monomer **2** as the carboxylate recognition site. The supplementary primary amine containing monomer **3** we reasoned would serve the 2-fold role of catalyzing the esterification and electrostatically stabilizing the carboxylate group (Figure 2).

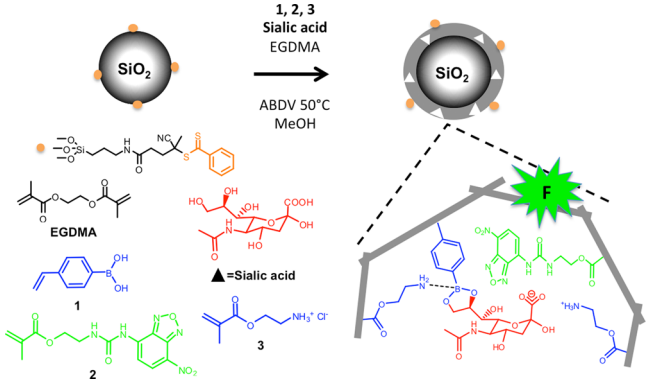

Figure 2. Procedure for RAFT-mediated grafting of a SA-imprinted shell on silica core particles by a mixed covalent and noncovalent approach based on reversible amine catalyzed boronate esterification (**1**,**3**), hydrogen bond stabilization through a guest-responsive fluorescent reporter group (**2**) and electrostatic stabilization (**3**).

RESULTS AND DISCUSSION

To verify the anticipated interactions, we carried out studies of the complexes with both SA and GA by ^{1}H NMR and UV/vis absorption and fluorescence spectroscopy. SA and GA are both pyranuronic acids but with different acid dissociation constants (pK_a = 2.6 and 3.7, respectively) and propensity for binding to phenylboronic acid.[15] A first indication of ternary and quarternary complex formation was obtained by considering the individual components' solubility in the polymerization solvent methanol (Figure 3).

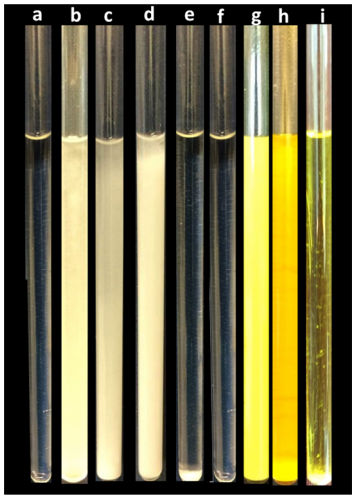

Figure 3. Photography of NMR tubes containing individual or combinations of SA-MIP prepolymerization components (C_{SA} = C_1 = C_2 = 1/2 × C_3 = 34 mM) in methanol. The tubes contained from left to right: (a) **1**; (b) SA+**1**; (c) SA+**3**; (d) SA; (e) SA+**1**+**3**; (f) **1**+**3**; (g) **2**; (h) SA+**2**; and (i) SA+**1**+**2**+**3**.

Whereas SA alone or in combination with **3** displayed limited solubility, this was enhanced in the presence of **1** and interestingly complete when all components (**1**+**3** or **1**+**2**+**3**) were present. Notably, we refrained from the addition of base because arylureas are susceptible to deprotonation under these conditions. The absorption and emission maxima of **2** in the presence or absence of the other components of the prepolymerization mixture remained centered at 411 ± 1 and 509 ± 1 nm (Figure S1), identical to the data in pure methanol, and further tests using solvatochromic dyes (Scheme S1) confirmed the polarity to be close to that of this solvent (Table S1). The absorption spectra of **2** also show only minor modulations in intensity, ±5%, whereas the fluorescence intensity undergoes more pronounced changes (Figure 4, Figures S1−S3). This indicates the presence of hydrogen-bonded species involving the various components. The study of SA and GA alone indicates GA to be a stronger hydrogen-bond acceptor interacting more strongly with **2** than SA; this is in line with their relative pK_a values (vide supra).[26] The situation reverses in the presence of **1** resulting in larger fluorescence enhancements for SA than for GA, possibly reflecting the relative stability of the respective phenylboronate esters in neutral buffer.[15] The results obtained with solvatochromic dye P2 support these findings (SI section 2, Figure S2, Table S1).

The ^{1}H NMR complexation-induced shifts also supported the presence of higher order complexes. Minor shift displacements (<0.01 ppm) were observed for most protons of **1**, **2**, and **3** when present in binary mixtures with one of the other

DOI: 10.1021/jacs.5b08482
J. Am. Chem. Soc. XXXX, XXX, XXX−XXX

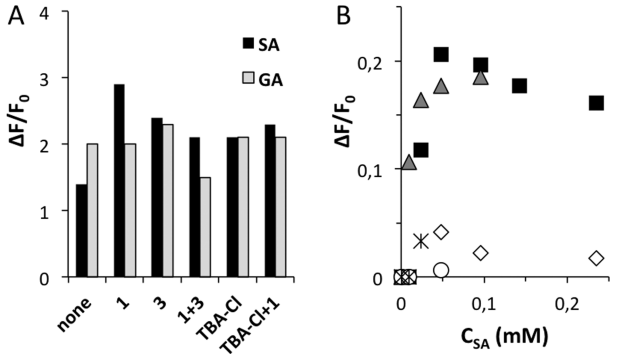

Figure 4. (A) Modulation of the fluorescence intensity of **2** in the presence of the prepolymerization components used for preparing the SA-MIP or GA-MIP (λ_{exc} = 411 nm; λ_{em} = 509 nm). None refers to equimolar additions of SA or GA and **2** (5 μM) in the presence of EGDMA in methanol. (B) Fluorescence enhancement measured for the SA-MIP versus concentration of SA in 2% (◇), 30% (■), 50% (gray ▲), 75% (×), and 98% (○) water.

monomers (e.g., **1**+**3**) (Tables S2–S4). These increased in the presence of SA (>0.01 ppm) and were maintained or increased further for the ternary and quarternary mixture.

SA- and GA-imprinted copolymers of monomer **1**–**3** and EGDMA were then grafted by reversible addition–fragmentation chain transfer (RAFT) polymerization[24,27] from the surface of 200 nm sized silica core particles (Figure 2) with a molar feed ratio of SA(GA):**1**:**2**:**3**:EGDMA equal to 1:1:1:2:20 and with the beads dispersed in methanol. After washing and template removal by acidic extractions, the beads were characterized by FTIR, TEM, and elemental analysis. The FTIR spectra of the core–shell beads shown in Figure S5 display two characteristic bands, that is, the carbonyl stretching of the polymer matrix at ca. 1740 cm^{-1} and the siloxane vibration of silica core at ca. 1120 cm^{-1}. As expected, the ratio of these band intensities scales with the density of grafted polymer, all in all indicating a successful grafting of the polymer shell with a slightly lower grafting yield for the SA-MIP. TEM images confirmed the core–shell architecture with shells appearing brighter due to their lower electron density (Figure S4). The shell thickness can be estimated to 10–20 nm, which is in rough agreement with the nominal thickness estimated by elemental analysis (10–13 nm) (Table S5), the GA-MIP featuring a slightly thicker shell than the SA-MIP. The images further revealed that the particles were polydisperse and present in separate or loosely aggregated form.

The particles were subsequently tested for their affinity toward the templates SA or GA in methanol–water mixtures. Binding curves were constructed (Figure S6) by plotting the specific amount of bound solute against the free concentration of solute determined by reversed phase HPLC. The corresponding fitting parameters (Table 1) reveal that the SA MIP exhibits an exceptionally strong affinity for SA, whereas the GA MIP binds its template more weakly.

Both the SA and the GA MIPs displayed selectivity for their templates, but the former showed by far the highest affinity and binding capacity. This relative binding affinity agrees with the spectroscopic characterization and the overall binding affinity of phenylboronic acid for these two sugars.[15] Interestingly, only the SA-MIP displayed binding associated fluorescence enhancement but only in 30% and 50% water (Figure 4B). In addition, no enhancements were observed using the GA-MIP probe (Figure S7). These curves displayed saturation at concentrations in agreement with the binding curves, confirming that the urea group is involved in the binding interactions at the imprinted site.

Table 1. Binding Constants (K) and Capacity (B_{max}) of Sialic Acid- and Glucuronic Acid-Imprinted Core–Shell Particles in Different Solvents

	sialic acid		glucuronic acid	
water (%)	K (M^{-1})	B_{max} (μmol g^{-1})	K (M^{-1})	B_{max} (μmol g^{-1})
2	6.6×10^5	12.0	3.3×10^4	13.3
50	3.5×10^4	9.0	2.1×10^4	8.2
98	5.9×10^3	8.4	1.8×10^3	10.7

To further map the binding selectivity of the imprinted receptor, we carried on with chromatographic tests of SA-imprinted microparticles. The latter were prepared analogously to the core–shell particles and were assessed as stationary phases for their retentivity for monosaccharides representative of the glycocalyx. As seen in Table 2, the SA-MIP showed a strong preference for SA with more than 80% of SA remaining column bound exceeding by nearly 3-fold the retention on a nonimprinted column. Particularly striking is the MIP's ability to discriminate between SA's of the human and animal types. Hence, the uptake of SA and *N*-glycolylneuraminic acid (gcSA) to the core–shell SA-MIP was 4.3 and 2.3 μmol/g, respectively, from 150 μM solutions of the sugars in water (2% methanol).

Table 2. Binding of Monosaccharides on SA-Imprinted and Nonimprinted Microparticles Expressed as % Bound (B) Based on HPLC Breakthrough Experiments[a]

monosaccharide	B_{MIP} (%)	B_{NIP} (%)
SA	84	34
gcSA	18	20
GA	20	10
Glc	13	<10
Gal	<10	<10
Fuc	<10	<10
GalNAc	24	19

[a]The values were calculated on the basis of the peak areas of peaks eluting within 25 min after injection.

We then moved on to probe the particles as imaging agents of cell lines featuring different expression levels of SA glycans. In cell imaging, the MIPs were evaluated for binding to SA on the prostate cancer cell lines DU145 and PC3, both known to express SA on the cell surface.[28] For comparison, an additional leukemic cell line, Jurkat T cells, was also studied. The cell membrane of DU145 cells was visibly stained within 60 min of SA-MIP addition, as shown in the fluorescence microscopy images (Figure S8A,B), whereas addition of the GA-MIP probe only produced weak cell staining, also upon prolonged incubation (Figure S8C,D).

This is in agreement with the low binding affinity displayed by the GA-MIP. The SA-MIP was hence used in the following imaging experiments.

To quantify the expression level of the sialic acid glycans, we used flow cytometry and a fluorescently labeled lectin (FITC-lectin), known to interact with sialic acids.[12,29] The result showed that the intensity of the probe reacted with DU145 and PC3 was higher than that of the other cell line (Figure 5, Figure S9). This agreed with previous expression analysis[28] of the level of sialic acid gangliosides in these prostate cancer cell lines. It

DOI: 10.1021/jacs.5b08482
J. Am. Chem. Soc. XXXX, XXX, XXX–XXX

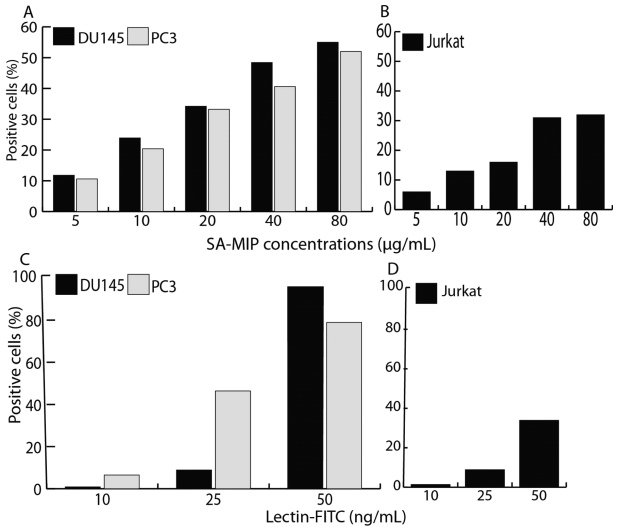

Figure 5. Flow cytometry-based quantification of cellular fluorescence of DU145 and PC3 cells (A,C) and Jurkat cells (B,D) as a function of added SA-MIP probe (A,B) or FITC-lectin (C,D) expressed as percent positive cells.

should be noted that SA-rich sites on nonactivated leukocytes, such as T and B cells, are masked by endogenous ligands and therefore not available for binding.[30]

We then turned to comparing these results with flow cytometry using the SA-MIP probe. As seen in Figure 5 and Figure S10, a similar pattern was observed as for the lectin stained cells with a significantly stronger staining of DU145 and PC3 as compared to the Jurkat cells.

By increasing the solution concentration of SA binding sites, the number of positive cells first increases but levels off at concentrations exceeding 40 μg mL^{-1}. Assuming the saturation capacity for SA from Table 1 and one type of binding sites, the association constants (K_a) between the SA-MIP and the glycan targets can be estimated (Table 3, Figure S11). These values exceed those for free SA (Table 1) as well as the affinity reported for other low molecular receptors interacting with cell surface glycans.[7]

Table 3. Binding Constants (K) and Maximum Degree of Cell Staining (S_{max}) of the Cell Lines Investigated in Figure 5

cell line	K (M^{-1})	S_{max} (%)
DU145	4.8 (±0.4) × 10^6	69
PC3	4.5 (±0.6) × 10^6	66
Jurkat	3.6 (±1.8) × 10^6	45

Combined with nuclear staining, the images showed that both probes stained the cells extracellularly in a qualitatively similar fashion despite the large difference in the nature and size of the probes (Figure 6). For the lectin, most of the probe appears bound on the cell surface, resulting in a ring-shaped fluorescence pattern appearing slightly more intense for the PC3 as compared to DU145 cells (Figure S9). This agreed with the behavior of SA-MIP, which also appeared to accumulate extracellularly on the surface of the cells. To further prove that the recognition ability of the SA-MIP involved the SA glycans, we exposed the cells to the glycosidase enzyme sialidase. This specifically removes SA from the cell surface. Thirty minutes of sialidase treatment (5 and 10 U mL^{-1}, respectively) led to clearly visible reduction in cell staining (Figure S12), providing

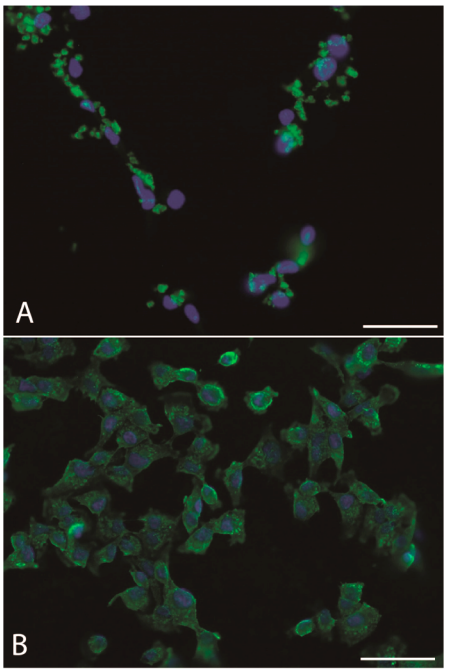

Figure 6. Fluorescence microscopy images of DU145 cells incubated in water (3% methanol) with SA-MIP (20 μg/mL) (A) and FITC-lectin (1 μg/mL) (B) after nuclear staining using DAPI (λ_{exc} = 359 nm; λ_{em} = 461 nm). Scale bar = 10 μm.

supporting evidence for the targeting ability of the SA-MIP. An important question is whether the SA-MIP staining is compatible with living cells. Figure S13 shows that the cells are effectively stained in fully biocompatible media such as PBS buffer, albeit at the expense of a slightly increased particle aggregation.

CONCLUSIONS

We have demonstrated a new ternary complex imprinting approach to produce tailor-made receptors with exceptional affinity for cell surface glycans. The affinity for sialic acid is on par with or exceeds the most powerful designed hosts reported to date comprising boronate hosts,[13,15] and hosts incorporating both urea and boronic acids.[10]

Moreover, the affinities compare favorably with those measured for lectins. Lectins bind only weakly to monosaccharides ($K \approx 10^3$ M^{-1}), whereas they interact more strongly with oligosaccharides or, as inherent in their multimeric structures, with several ligands through multivalent interactions.[31] This typically raises the affinity by 3−6 orders of magnitude. The SA-MIP behaves in a similar way. Thus, we observed a ca. 1000-fold enhanced affinity for the cell surface as compared to the free monosaccharide. As for lectins, we ascribe this to multivalent interactions with more than one cell surface SA binding to the probe, although microenvironmental effects cannot be excluded.

The presence of a fluorescent reporter group in the binding site suggests that light-up sensors for glycans can be designed along the principle we described in our previous report.[24] This will cancel out staining driven by nonspecific binding offering imaging probes with enhanced specificity for the targeted glycan. Moreover, as the results in Table 2 indicate, the application of the MIPs for targeted glycomics may be within reach. The above aspects are currently being explored.

DOI: 10.1021/jacs.5b08482
J. Am. Chem. Soc. XXXX, XXX, XXX−XXX

■ ASSOCIATED CONTENT

Supporting Information

The Supporting Information is available free of charge on the ACS Publications website at DOI: 10.1021/jacs.5b08482.

Experimental section reporting procedures for polymer synthesis and characterization; binding tests and cell imaging experiments and associated figures and tables (PDF)

■ AUTHOR INFORMATION

Corresponding Author

*borje.sellergren@mah.se

Present Address

[‖]Department of Organic and Biochemistry, Faculty of Chemistry, University of Tabriz, Tabriz 51666-14766, Iran.

Author Contributions

[⊥]S.S. and A.G.W. contributed equally.

Notes

The authors declare no competing financial interest.

■ ACKNOWLEDGMENTS

We gratefully acknowledge financial support from the Swedish Knowledge Foundation (grant no. 20120014) and an innovation project funded by BMWi/BAM.

■ REFERENCES

(1) *Essentials of Glycobiology*, 2nd ed.; Varki, A.; Cummings, R. D.; Esko, J. D.; et al., Eds.; Cold Spring Harbor Laboratory Press: Cold Spring Harbor, NY, 2009.

(2) Adamczyk, B.; Tharmalingam, T.; Rudd, P. M. *Biochim. Biophys. Acta, Gen. Subj.* **2012**, *1820*, 1347.

(3) Fuster, M. M.; Esko, J. D. *Nat. Rev. Cancer* **2005**, *5*, 526.

(4) Fujitani, N.; Furukawa, J.-i.; Araki, K.; Fujioka, T.; Takegawa, Y.; Piao, J.; Nishioka, T.; Tamura, T.; Nikaido, T.; Ito, M.; Nakamura, Y.; Shinohara, Y. *Proc. Natl. Acad. Sci. U. S. A.* **2013**, *110*, 2105.

(5) Cummings, R. D.; Etzler, M. E. In *Essentials of Glycobiology*; Varki, A., Cummings, R. D., Esko, J. D., et al., Eds.; Cold Spring Harbor Laboratory Press: Cold Spring Harbor, NY, 2009; Chapter 45.

(6) Neves, A. A.; Stöckmann, H.; Harmston, R. R.; Pryor, H. J.; Alam, I. S.; Ireland-Zecchini, H.; Lewis, D. Y.; Lyons, S. K.; Leeper, F. J.; Brindle, K. M. *FASEB J.* **2011**, *25*, 2528.

(7) Xu, X.-D.; Cheng, H.; Chen, W.-H.; Cheng, S.-X.; Zhuo, R.-X.; Zhang, X.-Z. *Sci. Rep.* **2013**, *3*, 10.1038/srep02679.

(8) Arnaud, J.; Audfray, A.; Imberty, A. *Chem. Soc. Rev.* **2013**, *42*, 4798.

(9) Jin, S.; Cheng, Y.; Reid, S.; Li, M.; Wang, B. *Med. Res. Rev.* **2010**, *30*, 171.

(10) Regueiro-Figueroa, M.; Djanashvili, K.; Esteban-Gómez, D.; de Blas, A.; Platas-Iglesias, C.; Rodríguez-Blas, T. *Eur. J. Org. Chem.* **2010**, 3237.

(11) Djanashvili, K.; Frullano, L.; Peters, J. A. *Chem. - Eur. J.* **2005**, *11*, 4010.

(12) Liu, A.; Peng, S.; Soo, J. C.; Kuang, M.; Chen, P.; Duan, H. *Anal. Chem.* **2011**, *83*, 1124.

(13) Yamamoto, M.; Takeuchi, M.; Shinkai, S. *Tetrahedron* **1998**, *54*, 3125.

(14) Frullano, L.; Rohovec, J.; Aime, S.; Maschmeyer, T.; Prata, M. I.; de Lima, J. J. P.; Geraldes, C. F. G. C.; Peters, J. A. *Chem. - Eur. J.* **2004**, *10*, 5205.

(15) Springsteen, G.; Wang, B. *Tetrahedron* **2002**, *58*, 5291.

(16) Wulff, G.; Sarhan, A.; Zabrocki, K. *Tetrahedron Lett.* **1973**, *14*, 4329.

(17) Wulff, G. *Angew. Chem., Int. Ed. Engl.* **1995**, *34*, 1812.

(18) Piletsky, S. A.; Piletskaya, E. V.; Yano, K.; Kugimiya, A.; Elgersma, A. V.; Levi, R.; Kahlow, U.; Takeuchi, T.; Karube, I.; et al. *Anal. Lett.* **1996**, *29*, 157.

(19) Kugimiya, A.; Yoneyama, H.; Takeuchi, T. *Electroanalysis* **2000**, *12*, 1322.

(20) Glad, M.; Norrloew, O.; Sellergren, B.; Siegbahn, N.; Mosbach, K. *J. Chromatogr.* **1985**, *347*, 11.

(21) (a) Bi, X.; Liu, Z. *Anal. Chem.* **2014**, *86*, 959. (b) Ye, J.; Chen, Y.; Liu, Z. *Angew. Chem., Int. Ed.* **2014**, *53*, 10386.

(22) Bie, Z.; Chen, Y.; Ye, J.; Wang, S.; Liu, Z. *Angew. Chem., Int. Ed.* **2015**, *54*, 10211.

(23) For a MIP-probe targeting hyaluronan see: Kunath, S.; Panagiotopoulou, M.; Maximilien, J.; Marchyk, N.; Sanger, J.; Haupt, K. *Adv. Healthcare Mater.* **2015**, *4*, 1322.

(24) Wan, W.; Biyikal, M.; Wagner, R.; Sellergren, B.; Rurack, K. *Angew. Chem., Int. Ed.* **2013**, *52*, 7023.

(25) Key, J. A.; Li, C.; Cairo, C. W. *Bioconjugate Chem.* **2012**, *23*, 363.

(26) Monomer **2** binds benzoate anion in chloroform with a binding constant of ca. 10^5 M^{-1} (see ref 24).

(27) Berghaus, M.; Mohammadi, R.; Sellergren, B. *Chem. Commun.* **2014**, *50*, 8993.

(28) Hatano, K.; Miyamoto, Y.; Nonomura, N.; Kaneda, Y. *Int. J. Cancer* **2011**, *129*, 1838.

(29) Cho, J.; Kushiro, K.; Teramura, Y.; Takai, M. *Biomacromolecules* **2014**, *15*, 2012.

(30) Razi, N.; Varki, A. *Glycobiology* **1999**, *9*, 1225.

(31) Ambrosi, M.; Cameron, N. R.; Davis, B. G. *Org. Biomol. Chem.* **2005**, *3*, 1593.

DOI: 10.1021/jacs.5b08482
J. Am. Chem. Soc. XXXX, XXX, XXX−XXX